OPTIMIZING THE DEPOSITION OF THIN LAYERS OF ORGANIC-INORGANIC HYBRID PEROVSKITE METHYLAMMONIUM LEAD IODIDE (CH3NH3PBI3) ON LARGE SURFACES THROUGH THEIR OPTICAL PROPERTIES

L. Ocaña[1], C. Quinto[1], C. Montes[1], A. Linares[2], E. Llarena[1], O. González[1], D. Molina[1], A. Pío[1],
C. Hernández-Rodríguez[3], S. González-Pérez[3] & R. Guerrero-Lemus[3], M. Friend[1] & M. Cendagorta[1].
[1]Instituto Tecnológico y de Energías Renovables, S. A. (ITER), Pol. Industrial de Granadilla, s/n, E 38600 Granadilla de Abona, España
Tlf. +34 922 747 700, Fax +34 922 747 701, E-mail. iter@iter.es
[2]Agencia Insular de Energía de Tenerife (AIET), Pol. Industrial de Granadilla, s/n, E 38600 Granadilla de Abona, España
Tlf. +34 922 747 700, Fax +34 922 747 701, E-mail. agenergia@agenergia.org
[3]Departamento de Física, Universidad de La Laguna, Avda. Astrofísico Fco. Sanchez s/n, 38200 La Laguna
Tenerife, Canarias, España.
Tfn: +34 922318243, Fax: +34 922318228, E-mail, chdezr@ull.edu.es

ABSTRACT: Nowadays, most of the Research and Development (R&D) efforts devoted to perovskite solar cells have been focused on achieving higher power conversion efficiencies, by using small sized substrates with even smaller active areas. The present paper proposes a method for optimizing the deposition of thin layers of organic-inorganic hybrid perovskite methylammonium lead iodide ($CH_3NH_3PbI_3$) on large surfaces (up to 75 mm x 75 mm) via spin coating procedures, performed in a clean room environment at room temperature and by considering their optical properties to assess their quality. Thus, in order to map the deposited area and realize studies about their optical properties, the absorption coefficient, the refractive index and layers thicknesses were determined by using a high accuracy spectroscopic ellipsometer system based on rotating compensator ellipsometer (RCE) technology from the J.A. Woolam Co. as functions of the wavelength, within a spectral range from 250 to 800 nm. Also, the samples were studied with a fluorescence spectroscopic system, in order to evaluate their photoluminescence properties and, in order to validate the chosen methodology; an Atomic Force Microscopy was used to verify the layers uniformity and thicknesses.
Keywords: Absorption, deposition, optical properties, photoluminescence.

1 INTRODUCTION

Since its foundation in 2009, the solar cell laboratory from Instituto Tecnológico y de Energías Renovables, S.A. (ITER) has been devoted to R & D on ways to optimize standard manufacturing processes of crystalline silicon solar cells [1]. In addition, a great deal of effort has been realized to extend its know-how to encompass other hot and emerging topics within the photovoltaic technologies. In this sense, Perovskite Solar Cells (PSC) has represented one of its main work activities during the last two years [2]. Throughout that time, the Department of Physics and the Research Support General Service (SEGAI) from the University of La Laguna have been key resources of technical support.

PSC emerged as a promising technology due to the rapidly increase in Power Conversion Efficiency (PCE) registered during the present decade, reaching a PCE record of 22.1% in 2016 [3]. Since most of the R&D efforts devoted to PSC have been focused on achieving higher PCE, by using small sized substrates with even smaller active areas [4], and several authors suggest the use of PSC as a top device in silicon-based tandem solar cells, due to the perovskite (PK) higher bandgap [5][6][7] and the appropriate refractive index [8][9][10], it is clearly necessary the study and optimization of deposition procedures that allow the implementation of PK films on larger substrates, aiming to converge this kind of technologies with the standard fabrication of crystalline solar cells.

The present paper evaluates the deposition of thin films of organic-inorganic hybrid perovskite composed by methylammonium lead iodide (MAPI) on large surfaces via spin coating techniques by considering their optical properties in order to assess their characteristics.

2 METHODOLOGY

All the fabrication procedures were performed in a clean room (ISO 7) environment at room temperature (~21 °C).

Initially the deposition of the PK thin films was undertaken on small size substrates (up to 25 mm x 25 mm) by spin coating from several PK solutions obtained by modifying the MAPI weight concentration. These films were evaluated in order to relate their optical properties with the literature [8][9]. The measurements were performed by mapping the substrate in order to acquire spatial resolution over the surface. In this sense, the refractive index, the extinction coefficient as well as the reflectance and transmittance rates were obtained by spectroscopic ellipsometry techniques as a function of the wavelength and for the film−substrate system. From these measurements, the absorption coefficient (α) and the refractive index (n) of the deposited films were calculated. Also, in order to better characterize the quality of the deposited layers, a FluoroSENS M-11 fluorometer [11] was used so as to determine its fluorescence properties.

Finally, the thickness of the deposited films was estimated from theoretical fit models, implemented by the ellipsometer system software, and evaluated by comparing the obtained results with measurements performed in parallel with an Atomic Force Microscope (AFM) [12].

From these trials, conclusions on the quality of the deposited layers were drawn and, since the objective for this paper was to evaluate the deposition of PK thin layers on larger substrates, the corresponding fabrication parameters were applied to produce and characterize substrates of bigger size.

3 EXPERIMENTAL

3.1 Study over small substrates

For the purpose of studying the PK depositions through their optical properties [8][9], the variables chosen were the weight concentration of the MAPI solutions and the spin coater acceleration. Thus, 25 wt% and 45 wt% MAPI solutions were deposited on 25 mm × 25 mm, 2 mm thick glass substrates, see Figure 1, setting the spin speed to 5000 rpm [7] while varying the acceleration parameter in 2000 rpm/s and 5000 rpm/s.

The relative humidity (RH) inside the chamber of the spin coating equipment was continuously monitored in order to perform the depositions when the Clean Dry Air (CDA) used by the device provided 10% RH within the chamber.
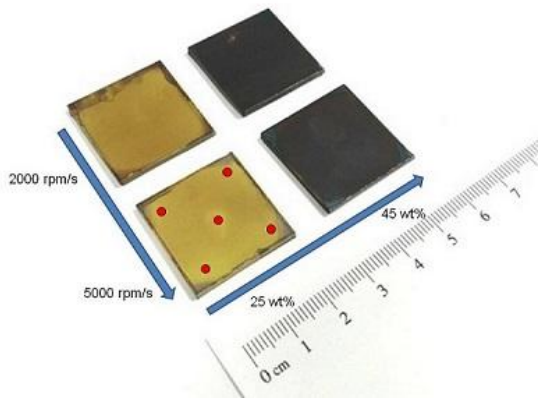

Figure 1: PK thin films deposited on 25 mm × 25 mm substrates, highlighting the measurement points (red dots).

Finally, in order to obtain the necessary spatial resolution, a matrix of measurement points was chosen as a system of reference for all the deposited samples, as it can be seen in Figure 1, in which the red dots represent the considered measurement points.

The samples were characterized, in ambient conditions, under a spectroscopic ellipsometer system composed by a 75 W Xe arc lamp, the beam collimation optics, a fixed polarizer and a compensator located in a continuously rotating motor at the entry arm. The receiver unit at the exit arm consists of a stepper motor driven rotational stage which houses an analyzer. In general, experimental measurements in ellipsometry define the ellipsometric parameters Ψ and Δ. These parameters were then used to calculate, from the theoretical fit models implemented by the data processing software CompleteEASE from J.A. Woolam Co, the refractive index (n), the extinction coefficient (k), the reflectance (R) and the transmittance (T) as functions of the wavelength (λ), as well as the average thickness of the deposited films [13].

3.2 Study over larger substrates.

Glass substrates with sizes 75 mm × 75 mm x 2 mm were chosen and spin coated with the 45 wt% MAPI solution by setting the speed to 5000 rpm, while trying two types of accelerations: 2000 rpm/s and 5000 rpm/s, as it was done in the previous section.
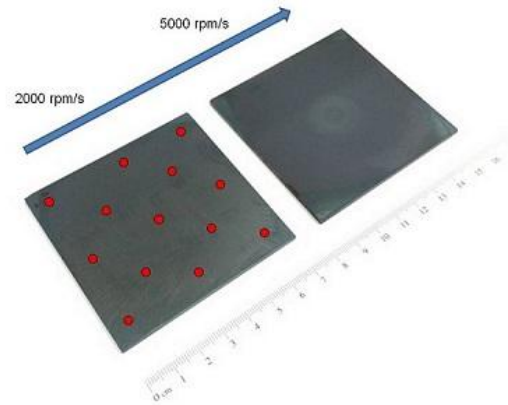

Figure 2: PK thin films deposited on 75 mm × 75 mm substrates, highlighting the measurement points (red dots).

Although visually the deposited samples showed a less uniform appearance, the ellipsometry study was performed by taking measurements in a matrix of equally spaced dots, following the same kind of pattern chosen for the smaller sized ones, as it can be seen in Figure 2 (red dots).

4. RESULTS AND DISCUSSION

4.1 Small substrates

For the purpose of studying the PK depositions through their optical properties [8][9], the variables chosen were the weight concentration of the MAPI solutions and the spin coater acceleration. Thus, 25 wt% and 45 wt% MAPI solutions were deposited on 25 mm × 25 mm, 2 mm thick glass substrates, see Figure 1, setting the spin speed to 5000 rpm [7] while varying the acceleration parameter in 2000 rpm/s and 5000 rpm/s.

The theoretical fit model was derived from the parameterization of the complex dielectric function by using the B-spline function, commonly used for the analysis of the optical constants for absorbing thin layers [13] in the visible range of the spectrum. Optical constants reported in the literature [8][9] were used as control points to match throughout the calculus. Thus, the obtained data was evaluated in a spectral range from 250 to 800 nm to define the material behavior over the visible range with a high degree of precision.

The absorption coefficient (α) for each processed sample was calculated from k, according to the Lambert's Law defined in eq. (1)

$$\alpha = \frac{4 \cdot \pi \cdot k}{\lambda} \qquad \text{eq.(1)}$$

Figure 3 shows a graph depicting the values obtained for the absorption coefficient (α) from the different samples, together with values published in the literature. Thus, as it can be seen, the behavior of the 45 wt% solution processed samples coincides with the values reported by Löper et al [8], presenting the same kind of trend reported by Leguy et al [9], in which there is an increase in the values of the absorption coefficient from 300 nm on, peaking by 350 nm, followed by a pronounced decrease which attenuates between 450 and 500 nm. Alike, a 1.59 eV band gap value is observed, confirming results from literature [5]-[10].

It can also be observed the difference in shape of the curves from the 25 wt% solution processed samples, particularly in the range between the 500 to 800 nm, which suggest a better performance for these samples for the purposes of operating within such range, rather than as component of a tandem device.
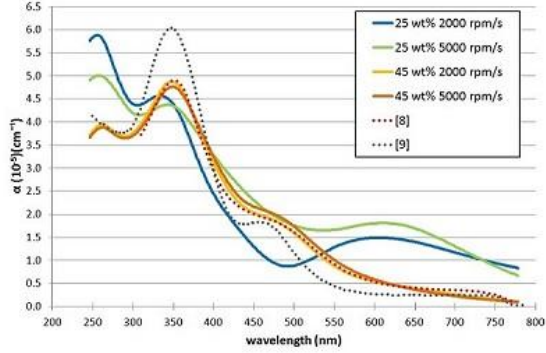

Figure 3: Absorption coefficient (α) of PK thin films deposited on 25 mm × 25 mm substrates.

Similarly, the values obtained for the refractive index (n) from the different samples were compared with the values published in the literature [8][9] and displayed in Figure 4. As it can be seen, the shape of the curves from the 45 wt% solution processed samples, follow a similar patron to the ones available, presenting two peaks clearly visible: one at 400 nm and the other between 500 and 550 nm. As to the curves of the 25 wt% processed samples, it can be seen how the first peak presents a softer shape, possibly due to a merging with the second one, and a rather diverging behavior from 450 nm onwards.
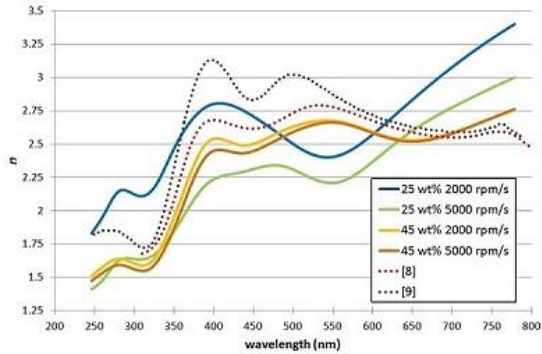

Figure 4: Refractive index (n) of PK thin films deposited on 25 mm × 25 mm substrates.

Regarding the value of the refractive index obtained for the 45 wt% solution processed samples at the wavelength of 633 nm, it is important to note that not only it was quite similar to the one published by Löper et al. [8] and Leguy et al [9] (that is, 2.53 versus 2.61 and 2.65, respectively), but also that it results a more suitable option for an Anti Reflective Coating (ARC) than standard photovoltaic manufacturing ones which, according to eq.(2) [14], addresses a value of 2.41.

$$n_1 = \sqrt{n_0 \cdot n_2} \qquad \text{eq.(2)}$$

Where n_0 is the refractive index of the surrounding material, 1.5 for encapsulant Ethyl Vinyl Acetate (EVA) [15], and n_2 is the refractive index of the semiconductor,

3.8763 for silicon [16].

From the values obtained by the spectroscopic ellipsometer, the reflectance and transmittance were also studied, this time, due to the sample positioning limitations given by the equipment, only at a determined point. As it can be seen in Figure 5, for both kinds of solutions, the reflectance remains stable between 0.20 and 0.30 points over one, from 330 nm to 800 nm, as it has been published [8][17][18]. As for the transmittance, near cero values were found from 330 nm to 360 nm for the 25 wt% solution processed samples, while for the 45 wt% ones the range extended form 330 nm to 500 nm, from where it begins to climb to 800 nm, reaching 0.80 points over one, a result that not only meet the values found in the literature [8][17][18], but also suggest the suitability of using this kind of deposited solutions as a better candidate for photovoltaic purposes.
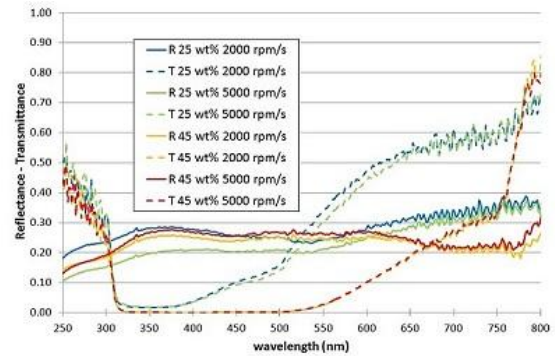

Figure 5: Reflectance and Transmittance versus wavelength of PK thin films deposited on 25 mm × 25 mm substrates.

In addition, as a way to evaluate the behavior of these thin film layers of perovskite when exposed to solar spectral irradiance, a study was performed following the approach described by Xie Ziang et al [10], by analyzing the conversion efficiency of these layers, without considering carrier recombination. This efficiency, known as *ideal efficiency*, is defined by eq. (3):

$$\eta = \frac{\int_0^{\lambda_g} I(\lambda) \cdot A(\lambda) \cdot \frac{\lambda}{\lambda_g} d\lambda}{\int_0^{\infty} I(\lambda) d\lambda} \qquad \text{eq.(3)}$$

Where $I(\lambda)$ is the solar intensity for a given range of wavelength (AM 1.5G) [19], $A(\lambda)$ is the absorptance ratio resulting from eq.(4):

$$A(\lambda) = 1 - R(\lambda) - T(\lambda) \qquad \text{eq.(4)}$$

λ is the wavelength and λ_g is the bandgap wavelength.

As it can be seen in Table I and Figure 6, the ideal efficiency obtained for the 45 wt% solution processed samples have a better response in the visible part of the spectrum than the 25 wt% ones, a result which also support their use as a better option for tandem devices together with crystalline silicon solar cells.

Table I: Ideal efficiency obtained for the PK thin films deposited on 25 mm × 25 mm substrates.

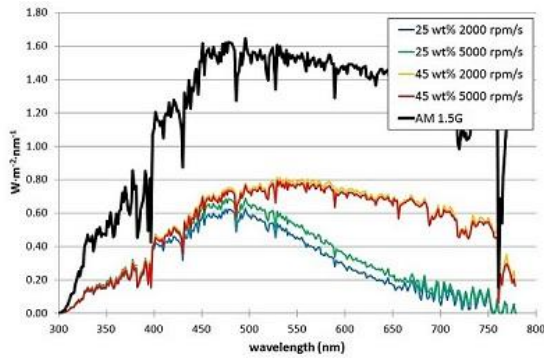| Solution (wt%)	Acceleration (rpm/s)	Substrate size (mm)	Ideal efficiency (η)
25	2000	25 × 25	23.78 %
25	5000	25 × 25	27.36 %
45	2000	25 × 25	45.81 %
45	5000	25 × 25	44.60 %

Figure 6: Ideal efficiency study of PK thin films deposited on 25 mm × 25 mm substrates.

On the other hand, in order to determine their fluorescence properties, the samples were studied with a fluorescence spectrometer, composed of two monochromators, a 75W Xenon lamp (THL) and a photo-multiplier tube (PMT) detector. The measurements were carried out by mapping the emission intensity for the samples over an excitation range. The excitation parameters were set from 300 to 800 nm, with 10 nm steps, and the emission ones were scanned from 300 to 800 nm, with an integrating time of 100 ms. In this way, it was possible to detect the wavelengths in which the excitation created conversion phenomena.

Figure 7 shows the results obtained for a 45 wt% solution processed sample, deposited at 5000 rpm/s. These results were quite similar for the rest of the samples, regardless of their weight concentration or the acceleration chosen during their deposition processes. As it can be seen, the higher emission intensity focuses on the visible range. However, some evidence of a conversion phenomenon also appears when the sample is excited between 350 and 400 nm, emitting between 700 and 800 nm.
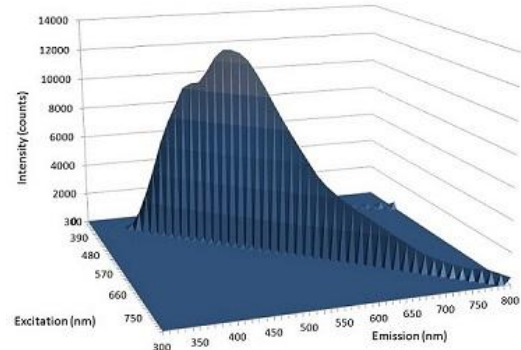

Figure 7: Excitation - Emission Mapping Scan of the sample with a 45wt% and an acceleration of 5000 rpm/s.

From these results, a further study of this phenomenon was carried out, this time by evaluating only the emission produced at different wavelengths from the excitation. In Figure 8 it can be observed, for the four cases studied, that a conversion took place when exciting the sample between 350 and 400 nm, resulting on an emission between 700 and 800 nm. This phenomenon has been extensity reported for organolead trihalide perovskites [20]-[27], although in these cases the excitation was carried out with a laser emitting at a wavelength of visible, and detecting an emission at around 760 nm.
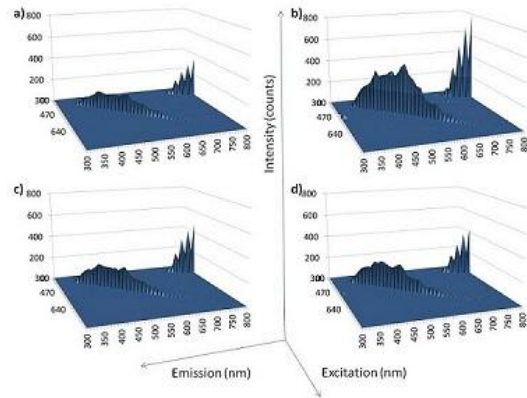

Figure 8: Excitation - Emission Mapping Scan of the sample: (a) Sample 25 wt% 2000 rpm/s, (b) Sample 25 wt% 5000 rpm/s, (a) Sample 45 wt% 2000 rpm/s and (a) Sample 45wt% 5000 rpm/s. The Z axis represents intensity in photon counting, the X axis excitation wavelength and the Y axis emission wavelength.

Table II summarizes the results obtained for the measured samples. By looking at these results, it can be concluded that the samples with 45 wt% have a higher conversion phenomenon than the 25 wt% ones and that, among the 45 wt% samples, the ones with higher acceleration have a slight better conversion as well. These results also support the suitability of using this kind MAPI layers in tandem with crystalline silicon solar cells.

Table II: Percentage of total conversion

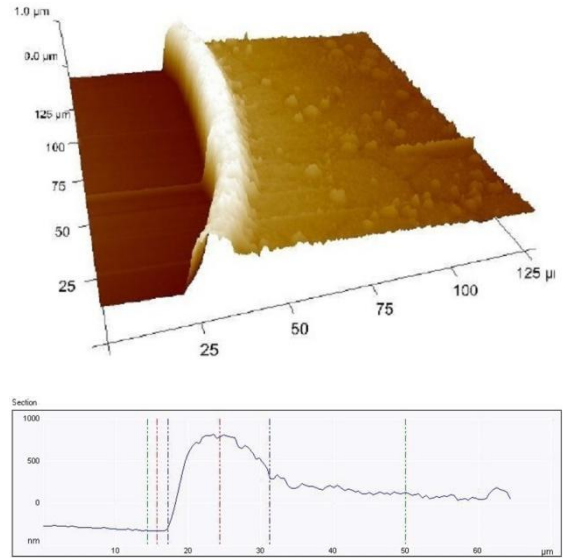| Solution (wt%)	Acceleration (rpm/s)	Substrate size (mm)	Total Conversion (%)
25	2000	25×25	2.33
25	5000	25×25	2.70
45	2000	25×25	2.87
45	5000	25×25	3.39

Finally, the average thickness was obtained by the theoretical fit model with the ellipsometer, as well as the resulting standard deviation for the 25 mm × 25 mm samples, as it can be seen summarized in Table III. There, it is shown that the approximate thickness for 25 wt% and 45 wt% processed samples was 255 nm and 435 nm respectively. These results confirm the dependence that exists between the solution weight concentration and the resulting deposited thickness [7]. Also, by considering the differences regarding the values obtained for the thickness standard deviation over the studied surfaces, it was possible that the 45 wt% were distributed around the mean value more closely than the 25 wt% ones, which suggest a better uniformity in the deposition processes.

Table III: Deposited thickness estimated by the ellipsometer fit model.

Solution (wt%)	Acceleration (rpm/s)	Substrate size (mm)	Average thickness (nm)	Standard deviation (nm)
25	2000	25×25	250.82	43.97
25	5000	25×25	262.81	63.16
45	2000	25×25	439.07	3.25
45	5000	25×25	432.15	4.37

As a way to confirm the validity of the results displayed in Table III, a set of samples were measured by both, the spectroscopic ellipsometer by way of the applied fit model, and a Atomic Force Microscope (AFM) [12]. Given the special requirements of the AFM measurement techniques, these samples were prepared by covering determined areas of the substrate with a polyimide tape before depositing the MAPI solution (45 wt%, with 5000 rpm and 5000 rpm/s as the setups for the wafer spinner). In this way, after peeling off the tape, the samples were ready for measuring the interface between the MAPI and the MAPI-free parts over the substrates.
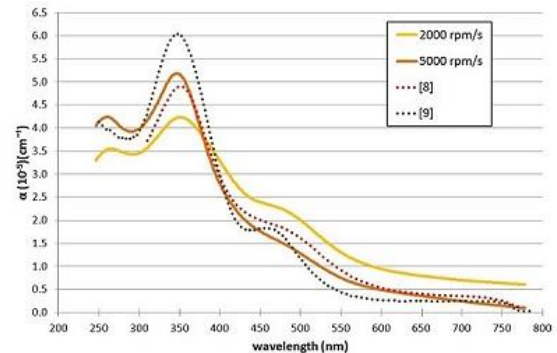
Figure 9 is an image from the AFM, depicting the interface between the MAPI and the MAPI-free areas. As it can be seen, at the MAPI side, although there is a sort of overgrowth or elevation around 1 μm thick, due to the impact of the MAPI solution against the border of the polyimide tape during the deposition, such effect fades further into the MAPI side and the thickness stabilizes at around 450 nm, a result that concurs with the values obtained by the ellipsometer.

Figure 9: AFM image and cross section, showing the interface between the MAPI-free and MAPI areas in one sample.

Taking into consideration all the above, the 45 wt% MAPI solution was chosen as the most suitable candidate to be evaluated over larger substrates.

4.2 Larger substrates.

As it can be seen in Figure 10, the values derived for the absorption coefficient (α) related to the samples deposited with an acceleration of 5000 rpm/s followed a pattern closest to both, the values obtained for smaller substrates, and the ones reported in the literature [8][9]. This was also true for the refractive index (n), as it can be seen in Figure 11, which shows a slight deviation from the reported behavior that increases considerably at higher wavelengths. Thus, the value obtained for 633 nm was 2.31, which evidences a value not as good as the one obtained for smaller substrates.

Figure 10: Absorption coefficient (α) of 45 wt% MAPI thin films deposited on 75 mm × 75 mm substrates.
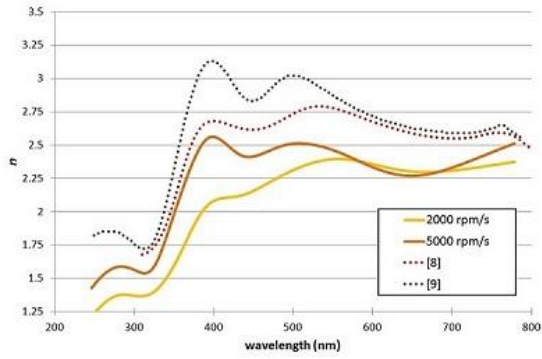
Figure 11: Refractive index (*n*) for 45 wt% MAPI solution deposited on 75 mm × 75 mm substrates.

Figure 12 shows that both, the transmittance and reflectance obtained for the 75 mm x 75 mm deposited substrates are worse than their respective values obtained for the smaller ones (and reported in the literature [8][17][18]). This can also be addressed as to a worsening in the uniformity of the deposited layers, which suggest the need for a better adjustment in the setting parameters for the wafer spinner, possibly in the line of increasing the acceleration.
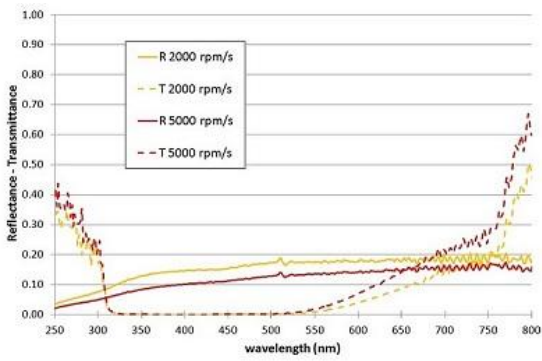

Figure 12: Reflectance and Transmittance versus wavelength of PK thin films deposited on 75 mm × 75 mm substrates.

Table IV and Figure 13 shows that the *ideal efficiency* values obtained for the 75 mm x 75 mm deposited substrates were quite similar to those obtained for the smaller ones with the same weight concentration. If any, they appear to have an even greater efficiency in the visible range, which decrease by the bandgap wavelength. Although this improvement seems to contradict the obtained values for the absorption coefficient, which correlated with worse deposition uniformity, it could be explained by the inherent simplicity of the theoretical approach, as per eq. (3).

Table IV: Ideal efficiency obtenied for the PK thin films deposited on 75 mm × 75 mm substrates.

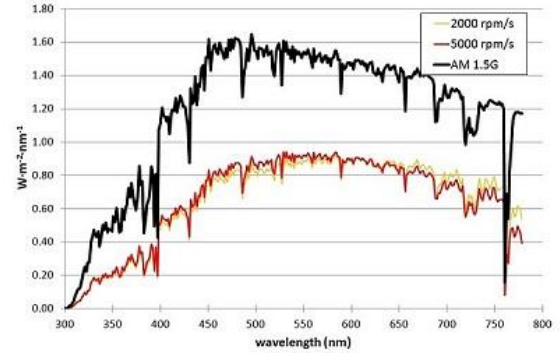| Solution (wt%)	Acceleration (rpm/s)	Substrate size (mm)	Ideal efficiency (η)
45	2000	75 × 75	55.02 %
45	5000	75 × 75	55.07 %

Figure 13 Ideal efficiency study of PK thin films deposited on 75 mm × 75 mm substrates.

Finally, Table V summarizes the results obtained by the ellipsometer fit model for the average thickness, together with their corresponding standard deviation.

Table V: Deposited thickness estimated by the ellipsometer fit model.

Solution (wt%)	Acceleration (rpm/s)	Substrate size (mm)	Average thickness (nm)	Standard deviation (nm)
45	2000	75 × 75	397.21	141.12
45	5000	75 × 75	478.55	117.05

By looking at the resulting data, although for the two accelerations the average thickness roughly corresponds to the values obtained for smaller substrates, their standard deviation was significantly worse, indicating a decrease on the uniformity for the deposited layers, a result which concurs with the visual assessment as it was stated previously. Still and all, these results seem to indicate a possible way for improving the uniformity of the deposited layers by applying higher accelerations.

5. CONCLUSIONS

The use of a spectral ellipsometer as a characterization method for evaluating the optical properties as well as the thickness of thin films of perovskite, deposited over substrates of different sizes, has been demonstrated. This has been achieved by applying a theoretical fit model derived from the parameterization of the complex dielectric function via the use of the B-spline function and by adjusting the calculus in order to comply with the optical constants reported in the literature.
Form the two kinds of MAPI solutions studied, the samples produced with 45 wt% ones were found as a better option for being used not only as an alternative Anti Reflecting Coating material, but also as an active member of a tandem solar cell, together with crystal silicon substrates. This conclusion was sustained by studying their optical properties, such as the absorption coefficient, refraction index, transmittance, reflectance, ideal efficiency and fluorescence properties.
The thickness and uniformity of the resulting deposited samples via spin wafer has been studied over substrates of 25 mm × 25 mm and 75 mm x 75mm and conclusions were obtained for improvement as sizes increase.

6. REFERENCES

[1] Quinto C.; Ocaña L.; Montes C.; Linares A.; Llarena E.; González-Díaz B.; González-Pérez S.; Guerrero-Lemus R., Friend M.; Cendagorta M. Design, start up and society benefits of a PV solar cell laboratory, 30th European Photovoltaic Solar Energy Conference and Exhibition 2014, Amsterdam, Netherlands, doi: 10.4229/EUPVSEC20142014-7AV.6.56

[2] Ocaña L.; Linares A.; Llarena E.; Montes C.; Gózález O.; Molina D.; Pío A.; Quinto C.; Friend M.; Cendagorta M. Adaptation of a Crystalline Silicon Solar Cell Laboratory to Produce Perovskite Solar Devices, 31st European Photovoltaic Solar Energy Conference and Exhibition 2015, Hamburg, Germany, doi: 10.4229/EUPVSEC20152015-3BV.5.40

[3] National Renewable Energy Laboratory (NREL) Best Research-Cell Efficiencies Chart. Access: May 2016 http://www.nrel.gov/ncpv/images/efficiency_chart.jpg

[4] Fan J.; Jia B.; Gu M. Perovskite-based low-cost and high-efficiency hybrid halide solar cells, Photon Res. 2014 2 111-120, doi: 10.1364/PRJ.2.000111

[5] Löper, P.; Niesen, B.; Moon, S.; Martin de Nicolas, S.; Holovsky, J.; Remes, Z.; Ledinsky, M.; Haug, F.; Yum, J.; De Wolf, S.; Ballif, C. Organic-Inorganic Halide Perovskites: Perspectives for Silicon-Based Tandem Solar Cells. IEEE J. Photovoltaics 2014, 4, 1545−1551, doi: 10.1039/c4cp03788j

[6] Mailoa J.; Bailie C.; Johlin E.; Hoke E.; Akey A.; Nguyen W.; McGehee M.; Buonassisi T. A 2-terminal perovskite/silicon multijunction solar cell enabled by a silicon tunnel junction, Appl. Phys. Lett. 2015, 106, 121105, doi:10.1063/1.4914179

[7] Xiao, M., Huang, F., Huang, W., Dkhissi, Y., Zhu, Y., Etheridge, J., Gray-Weale, A., Bach, U., Cheng, Y.-B. and Spiccia, L. A Fast Deposition-Crystallization Procedure for Highly Efficient Lead Iodide Perovskite Thin-Film Solar Cells, Angew. Chem. Int. Ed. 2014 53: 9898–9903. doi:10.1002/anie.201405334

[8] Löper, P.; Stuckelberger M.; Niesen, B.; Werner J.; Filipič W.; Moon, S.; Yum, J.; Topič M.; De Wolf, S.; Ballif, C. Complex Refractive Index Spectra of CH3NH3PbI3 Perovskite Thin Films Determined by Spectroscopic Ellipsometry and Spectrophotometry, The Journal of Physical Chemistry Letters 2015 6 (1), 66-71, doi: 10.1021/jz502471h

[9] Leguy A.; Hu Y.; Campoy-Quiles M.; Alonso M., Weber O.; Azarhoosh P.; Schilfgaarde M.; Weller M.; Bein T.; Nelson J.; Docampo P.; Barnes P., Reversible Hydration of CH3NH3PbI3 in Films, Single Crystals, and Solar Cells, Chemistry of Materials 2015 27 (9), 3397-3407 doi: 10.1021/acs.chemmater.5b00660

[1] Ziang X.; Shifeng L.; Laixiang Q.; Shuping P.; Wei W.; Yu Y.; Li Y.; Zhijian C.; Shufeng W.; Honglin D.; Minghui Y.; Qin G. Refractive index and extinction coefficient of CH3NH3PbI3 studied by spectroscopic ellipsometry, Opt. Mater. Express 2015 5, 29-43, doi: 10.1364/OME.5.000029

[11] FluoroSENS M-11, modular fluorimeter. Laser Technology S.L., Barcelona, Spain.

[12] Atomic Force Microscope (AFM), model Nanoscope III Multimode by Digital Instrument (Santa Barbara, California) available at the Atomic Force Microscope Service, within the Research Support General Service, integrated in the University of La Laguna.

[13] J.A. Woolam Co., Ellipsometry FAQ. Access: May 2016. https://www.jawoollam.com/resources/ellipsometry-faq

[14] Zhao J.; Green M. Optimized antireflection coatings for high-efficiency silicon solar cells, IEEE Transactions on Electron Devices 1991 vol. 38, no. 8, pp. 1925-1934, doi: 10.1109/16.119035

[15] McIntosh K.; Cotsell J.; Cumpston J.; Norris A.; Powell N.; Ketola B. An optical comparison of silicone and EVA encapsulants for conventional silicon PV modules: A ray-tracing study, 34th IEEE Photovoltaic Specialists Conference (PVSC) 2009 Philadelphia, PA, pp. 000544-000549. doi: 10.1109/PVSC.2009.5411624

[162] Green M.; Keevers M. Optical properties of intrinsic silicon at 300 K, Progress in photovoltaics 1995 3, 189-192, doi: 10.1002/pip.4670030303

[17] The Duong, Niraj Lal, Dale Grant, Daniel Jacobs, Peiting Zheng, Shakir Rahman, Heping Shen, Matthew Stocks, Andrew Blakers, Klaus Weber, Thomas P. White, and Kylie R. Catchpole, "Semitransparent Perovskite Solar Cell With Sputtered Front and Rear Electrodes for a Four-Terminal Tandem". IEEE JOURNAL OF PHOTOVOLTAICS

[18] Yajie Jiang , Martin A. Green, Rui Sheng, Anita Ho-Baillie, "Room temperature optical properties of organic–inorganic lead halide perovskites". Solar Energy Materials & Solar Cells, Volume 137, June 2015, Pages 253–257

[19] Air Mass 1.5 Direct+Circumsolar spectrum, American Society for Testing and Materials: http://rredc.nrel.gov/solar/spectra/am1.5/)

[20] Haiping He, Qianqian Yu, Hui Li, Jing Li, Junjie Si, Yizheng Jin, Nana Wang, Jianpu Wang, Jingwen He, Xinke Wang, Yan Zhang & Zhizhen Ye. "Exciton localization in solution-processed organolead trihalide perovskites". Nature communications. Published 21 Mar 2016. DOI: 10.1038/ncomms10896

[21] Michele Saba, Michele Cadelano, Daniela Marongiu, Feipeng Chen, Valerio Sarritzu, Nicola Sestu, Cristiana Figus, Mauro Aresti, Roberto Piras, Alessandra Geddo Lehmann, Carla Cannas, Anna Musinu, Francesco Quochi, Andrea Mura & Giovanni Bongiovanni. "Correlated electron–hole plasma in organometal perovskites". Nature communications. Published 30 Sep 2014. DOI: 10.1038/ncomms6049

[22] Son-Tung Ha, Chao Shen, Jun Zhang and Qihua Xiong. "Laser cooling of organic–inorganic lead halide perovskites". Nature Photonics. PUBLISHED ONLINE: 21 DECEMBER 2015. DOI: 10.1038/NPHOTON.2015.243

[23] Christian Wehrenfennig, Mingzhen Liu, Henry J. Snaith, Michael B. Johnston, and Laura M. Herz. " Homogeneous Emission Line Broadening in the Organo Lead Halide Perovskite CH3NH3PbI3−xClx". Physical Chemistry Letters. Published 24 Mar 2014. dx.doi.org/10.1021/jz500434p | J. Phys. Chem. Lett. 2014, 5, 1300−1306

[24] Zhi-Kuang Tan, Reza Saberi Moghaddam, May Ling Lai, Pablo Docampo, Ruben Higler, Felix Deschler, Michael Price, Aditya Sadhanala, Luis M. Pazos, Dan

Credgington, Fabian Hanusch, Thomas Bein, Henry J. Snaith and Richard H. Friend. "Bright Light-Emitting Diodes based on Organometal Halide Perovskite". Nature Publishing Group, 1748-3387, dx.doi.org/10.1038/nnano.2014.149.

[25] Aditya Sadhanala, Felix Deschler, Tudor H. Thomas, Sian E. Dutton, Karl C. Goedel, Fabian C. Hanusch, May L. Lai, Ullrich Steiner, Thomas Bein, Pablo Docampo, David Cahen,§ and Richard H. Friend. "Preparation of Single-Phase Films of CH3NH3Pb(I1−xBrx)3 with Sharp Optical Band Edges". dx.doi.org/10.1021/jz501332v | J. Phys. Chem. Lett. 2014, 5, 2501−2505

[26] Meng Zhang, Hua Yu, Miaoqiang Lyu, Qiong Wang, Jung-Ho Yun and Lianzhou Wang. "Composition-dependent photoluminescence intensity and prolonged recombination lifetime of perovskite CH3NH3PbBr3−xClx films". Chem. Commun., 2014,50, 11727-11730. DOI: 10.1039/C4CC04973J

[27] Michele Cadelano, Michele Saba, Nicola Sestu, Valerio Sarritzu, Daniela Marongiu, Feipeng Chen, Roberto Piras, Francesco Quochi, Andrea Mura and Giovanni Bongiovanni. "Photoexcitations and Emission Processes in Organometal Trihalide Perovskites". http://dx.doi.org/10.5772/61282